HEP'97 #546
Submitted to Pa 2, 4
Pl 1, 2, 4

DELPHI 97-117 CONF 99
20 July, 1997

Scaling Violation in Quark and Gluon Jets

Preliminary

DELPHI Collaboration

K. Hamacher, O. Klapp, P. Langefeld, M. Siebel
University of Wuppertal, Germany

Abstract

The fragmentation function of quarks and gluons is measured in various three-jet topologies in Z decays collected with the DELPHI detector between 1991 and 1994. The results are compared at different values of a transverse-momentum-like scale. Gluon jets are identified in three-jet events containing primary heavy quarks using impact parameter information. Comparable quark jet properties are obtained from light quark dominated three-jet events.
The scale dependence of the fragmentation functions of quark and gluon jets shows the pattern typical of scaling violations. The scaling violation for quark jets is similar to that observed for all events in e^+e^- annihilation while that for gluon jets appears to be significantly stronger.
The ratio of the logarithmic slopes of the fragmentation function for gluon to quark jets at large scaled hadron momentum allows a direct determination of the colour factor ratio C_A/C_F:

$$\frac{\frac{d\log D_{gluon}}{d\log\kappa}}{\frac{d\log D_{quark}}{d\log\kappa}} = 2.7 \pm 0.7(stat.)$$

Paper submitted to the HEP'97 Conference
Jerusalem, August 19-26

1 Introduction

The observation of the scaling violations of the deep inelastic nucleon structure function $F_2(x_{Bj}, Q^2)$ [1, 2], and later the complementary measurement of scaling violations of the quark fragmentation function $D_Q(x, Q^2)$ [3], are among the fundamental tests of Quantum Chromodynamics, QCD. Evidently it is interesting to extend these studies also to scaling violations in gluon fragmentation. The presence of scaling violations in gluon fragmentation directly proves the presence of the triple gluon coupling, one of the most basic ingredients of the non-abelian gauge theory QCD. Comparing scaling violations in quark and gluon fragmentation also allows the relative coupling strengths of gluon radiation from quarks and of the triple gluon coupling to be determined directly, as was demonstrated in a previous publication [7].

In this paper we present a detailed comparison of scaling violations in quark and gluon fragmentation.

Quark and gluon initiated jets are identified in symmetric and asymmetric three-jet events originating from hadronic Z decays. This increases the statistical precision compared to previous data based on symmetric topologies only. Gluon jets are identified using heavy quark tagging. Quark data are obtained from a quark gluon mixture, subtracting the corresponding gluon data.

The identification of quark and gluon jets relies on the analogy to tree level graphs. Higher order corrections affect this definition by terms of $\mathcal{O}(\alpha_S)$. The relevant scales are determined from the jet energies and the event topology, as in studies of the scale dependence of the multiplicity in quark and gluon jets [4, 5].

The paper is organized as follows. Section 2 describes shortly some technical aspects of the analysis. Section 3 contains some theoretical preliminaries and introduces the variables and distributions used for this study. The results are presented in section 4 and compared to QCD calculations. The sensitivity of the results to the QCD colour factors C_A and C_F is discussed. Conclusions appear in section 5.

2 Data Analysis

A detailed description of the DELPHI apparatus has been presented in [6].

All data collected by DELPHI during the years 1991 to 1994 are considered in the present analysis. Cuts applied to charged and neutral particles and to events in order to select hadronic Z decays are identical to those given in [7, 8]. Three-jet events are clustered using the Durham-algorithm [10] with a jet resolution parameter $y_{cut} = 0.015$.

For a detailed comparison of quark and gluon jet properties it is necessary to obtain samples of quark and gluon jets with nearly the same kinematics and the same scales, to allow a direct comparison of the jet properties. To fulfill this condition, different event topologies have been used, as illustrated in Fig. 1:

- Basic three-jet events with $\theta_2, \theta_3 \in [135° \pm 35°]$.
- Mirror symmetric events, $\theta_2, \theta_3 \in (120°, 130°, 140°, 150°, 160°) \pm 5°$, subsequently called **Y events**. These Y events are a sub-sample of the basic three-jet events in which the two low-energy jets should be directly comparable.

The jet axes are projected into the event plane, which is defined as the plane perpendicular to the smallest sphericity eigenvector as obtained from the quadratic momentum

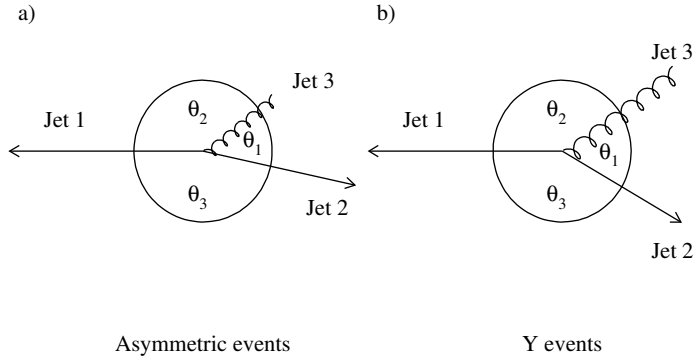

Figure 1: Event topologies of symmetric Y events and asymmetric events. θ_i are the angles between the jets after projection into the event plane.

tensor. The jets are numbered in decreasing order of jet energy, where the energy of each jet is calculated from the angles between the jets assuming massless kinematics:

$$E_j^{calc} = \frac{\sin\theta_j}{\sin\theta_1 + \sin\theta_2 + \sin\theta_3}\sqrt{s}, \qquad j = 1,2,3\,, \tag{1}$$

where θ_j is the interjet angle as defined in Fig. 1.

In order to enhance the contribution from events with three well-defined jets attributed to $q\bar{q}g$ production, further cuts are applied to the three-jet event samples, as in [7]. From the initial ~2,950,000 hadronic events collected by DELPHI in 91-94 and from ~6,360,000 Monte Carlo events, there remain ~60,000 symmetric and ~325,000 asymmetric events.

The identification of gluon jets by anti-tagging of heavy quark jets is identical to that described in [7, 11]. The efficiency and purity calculations have been made using events generated by the JETSET 7.3 Monte Carlo [12] tuned to DELPHI data [13], passed through the full simulation program (DELSIM [14, 15]) of the DELPHI detector and the standard DELPHI data reconstruction chain. Even in the Monte Carlo, the assignment of parton flavours to the jets is not unique, as in parton models like JETSET the decay history is interrupted by the building of strings (or clusters in the case of HERWIG). Thus three independent ways of defining the gluon jet in the fully reconstructed Monte Carlo are investigated [8, 9]:

- *angle assignment:* The gluon induced jet is assumed to be the jet making the largest angle with the nearest B-hadron originating from the primary b-quarks.
- *history assignment:* The jet containing the fewest decay particles from the heavy hadrons is assigned to the gluon.
- *PS assignment:* First the partons are clustered to three jets if the event is accepted as containing three well measured jets at detector level. Quarks are given a weight of +1, antiquarks a weight of −1, and gluons a weight of 0. Parton jets are identified as quark and gluon jets if the sum of the flavour weights of all partons in a certain parton jet is +1, -1, and 0, respectively. The small amount (2%) of events not showing this expected pattern were discarded. A gluon jet is identified as the parton jet which sum of the parton flavours yield 0. These parton jets are mapped onto the hadron jets in such a way that the sum of the angles between the three hadron jets and their belonging parton jets is minimized.

Method		Angle assignment		
	gluon in:	Jet 1	Jet 2	Jet 3
	Jet 1	4.5%	0%	0.03%
PS	Jet 2	0%	23.3%	0.3%
assignment	Jet 3	0.02%	0.13%	71.8%

Table 1: Correlation of angle and PS assignments. The table has been obtained for arbitrary three-jet events with $\theta_2, \theta_3 \in [90°, 170°]$. These events also contain the symmetric events.

Tab. 1 shows that for the angle and PS assignments give similar results and that therefore the purities can be estimated with small systematic uncertainties. As in Monte Carlo events the gluon jets can be identified in b-events and in light quark events with the PS assignments, this method is used rather than the hadron assignments. With the tagging procedure described in this section, gluon jet purities [1] from 40% to 90% are achieved, depending on the topology.

In order to achieve pure quark ($udsc$) and gluon jet distributions the data have been corrected using events simulated with JETSET 7.3. This is justified by the good agreement between data and simulation. Moreover, the effects of finite resolution and acceptance of the detector are corrected using a full simulation of the DELPHI detector. In the further analysis, topologies with a purity below 40% are not considered. Furthermore, bins with high acceptance correction factors are disregarded.

3 Theory

The fundamental QCD couplings are illustrated in Fig. 2.

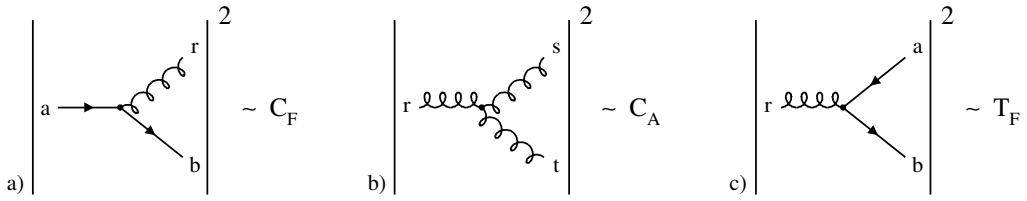

Figure 2: Diagrams of the fundamental QCD couplings

[1] Here the purity is defined as the ratio of the number of real tagged gluons (i.e. jets originating from gluons) to the total number of jets tagged as gluons.

Their relative coupling strength is determined by the colour factors (also called Casimir factors) which are determined by the structure of $SU(3)$, the group underlying QCD. The Casimir factors C_F, C_A, and T_F determine the coupling strengths of gluon radiation from quarks, of the triple-gluon vertex, and of gluon splitting into a quark-antiquark pair, respectively. Within $SU(3)$, these coupling constants are $C_F = 4/3$, $C_A = 3$, and $T_F = 1/2$, which has to be weighted by the number of active quark flavors n_F. Due to the quark masses, the actual value of active flavours n_F is energy dependent. At large energy (checked e.g. for the $150° \pm 5°$ topology), the JETSET model predicts $n_u \sim n_d \sim n_s \sim n_c \sim 2 \cdot n_b$, which corresponds to $n_F \simeq 4.5$, whereas in the low energy limit $n_F \simeq 3$.

3.1 Jet Scales

In order to scaling violations, the scale underlying the evolution of the corresponding jet needs to be known. Usually this is taken to be the centre of mass energy, E_{cm}. As all jets entering this analysis stem from Z decays, thus from fixed E_{cm} the scale has to be determined from the jet energy and the event topology. In the present study we restrict ourselves to use the so called hardness scale, κ_{DDT} [16] [2]:

$$\kappa^i_{DDT} = E^i_{calc} \cdot \sin \frac{\theta_{min}}{2} \tag{2}$$

where E^i_{calc} is the energy of jet i as determined by Eq. 1, and θ_{min} is the angle with respect to the closest jet. κ_{DDT} is similar to the transverse momentum of the jet and is also related to $\sqrt{y_{cut}}$, as used by the jet algorithms. Other scales, like the so called dipole scale, used by the ARIADNE Monte Carlo generator [17], which have been successfully applied to the study of the scale dependence of the multiplicity [5] will be included later.

Fig. 3 compares the distribution of the jet energies κ_E and hardnesses κ_{DDT} for the jets of the five symmetric event topologies.

The upper plot of Fig. 3 shows the distribution of the jet energies. As can be seen, there is a great overlap among the distributions, which implies that jets may have the same energy in spite of being taken from two different topologies. The lower plot shows the distributions of κ_{DDT}. The κ_{DDT} distributions are clearly separated for the different symmetric event topologies. This can be understood easily: in the case of symmetric events and massless jets, κ_{DDT} falls steeply to 0 with increasing $\theta_2 (= \theta_3)$, while the energy becomes nearly constant (see Fig. 3c). This makes κ_{DDT} less sensitive to small deviations from the exact symmetric topology than the energy itself. Finally it should be noted that the available range of scales is bigger in case of κ_{DDT} compared to the jet energy.

Tab. 2 shows the geometrical calculated and measured values of the different jet scale definitions for the symmetric topologies.

The agreement between the calculated and the measured mean values of κ is excellent, taking into account that since gluon radiation is a Bremsstrahlung effect θ_2 and θ_3 are shifted towards the higher limit of θ in a symmetric bin, thus yielding lower average values of κ.

[2] named after Dokshitzer, Diakonov and Trojan

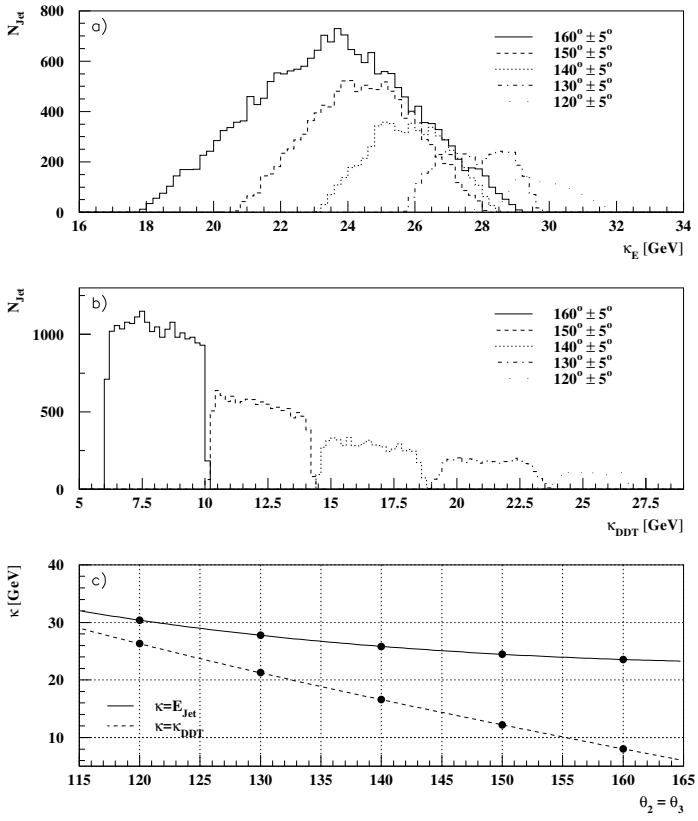

Figure 3: Separation of symmetric event topologies by the jet energy and hardness scales.

3.2 Scale Dependence of the Fragmentation Function of Quark and Gluon Jets

Jet splittings may be studied with respect to the energy sharing in a splitting process. This analysis is connected to the analysis of the scale dependence (scaling violation) of the fragmentation functions $D_p^H(x_E, s)$ of a parton p into a hadron H as described by the GDLAP [3] equations [18], where s is the relevant scale to be replaced by κ_{DDT}. In the limit of large hadron energy fractions $x_E = E_{hadron}/E_{jet}$, i.e. for $x_E \geq \frac{1}{2}$, the lower energy parton in a splitting process cannot contribute. In a $q \to qg$ splitting process the lower energy parton is almost always the gluon. The $g \to q\bar{q}$ splitting is disfavoured w.r.t. $g \to gg$. The (leading order) evolution equations for quarks and gluons therefore simplify to:

$$\frac{dD_g^H(x_E,s)}{d\ln s} = \frac{\alpha_s(s)}{2\pi} \cdot \int_{x_E}^1 \frac{dy}{y} P_{g\to gg}(\frac{x_E}{y}) \cdot D_g^H(y,s) \tag{3}$$

$$\frac{dD_q^H(x_E,s)}{d\ln s} = \frac{\alpha_s(s)}{2\pi} \cdot \int_{x_E}^1 \frac{dy}{y} P_{q\to qg}(\frac{x_E}{y}) \cdot D_q^H(y,s)\,. \tag{4}$$

[3] **G**ribov, **D**okshitzer, **L**ipatov, **A**ltarelli, and **P**arisi

	κ_E		κ_{DDT}		κ_{Dipole}	
Topology	calc.	meas.	calc.	meas.	calc.	meas.
120°	30.40	29.66	26.33	25.08	26.33	25.50
130°	27.76	27.64	21.26	21.11	23.13	22.98
140°	25.82	25.75	16.60	16.48	20.07	19.96
150°	24.44	24.21	12.22	11.96	16.98	16.72
160°	23.51	23.24	8.04	7.90	13.64	13.43

Table 2: κ values of the low energy jets in symmetric topologies.

The relevant Altarelli Parisi splitting kernels are:

$$\begin{aligned} P_{q\to qg}(z) &= C_F \cdot \frac{1+z^2}{1-z} \\ P_{g\to gg}(z) &= 2C_A \cdot \frac{(1-z(1-z))^2}{z(1-z)} \end{aligned}$$

For a quantitative comparison of gluon and quark fragmentation, it is important to compare the relative size of the observed scaling violation:

$$\mathcal{S}_p = \frac{d\ln D_p^H(x_E,s)}{d\ln s}, \tag{5}$$

Thus the following ratio is defined:

$$r_{\mathcal{S}}(x_E) = \frac{\mathcal{S}_g}{\mathcal{S}_q} = \frac{\frac{d\ln D_g^H(x_E,s)}{d\ln s}}{\frac{d\ln D_q^H(x_E,s)}{d\ln s}}.$$

This ratio can be predicted by solving the GDLAP equation numerically [19]. The following ansatz has been used to fit the fragmentation function at a fixed reference scale:

$$D_p^F(x_E) = p_3 \cdot x_E^{p_1} \cdot (1-x_E)^{p_2} \cdot \exp\left(-p_4 \cdot \ln {x_E}^2\right) \tag{6}$$

$r_{\mathcal{S}}$ can then be calculated as a function of x_E by solving the GDLAP equations. The limit $r_{\mathcal{S}}(x \to 1)$ is easily calculated:

$$r_{\mathcal{S}}(1) = \lim_{x_E\to 1} \frac{\frac{d\ln D_g^H(x_E,s)}{d\ln s}}{\frac{d\ln D_q^H(x_E,s)}{d\ln s}} = \frac{C_A}{C_F}. \tag{7}$$

Thus $r_{\mathcal{S}}$ can be used directly to measure $\frac{C_A}{C_F}$. Experimentally $r_{\mathcal{S}}(x_E)$ is accessible by measuring the ratio of the slopes of the $D_p^F(x_E,s)|_{x_E}$ curves.

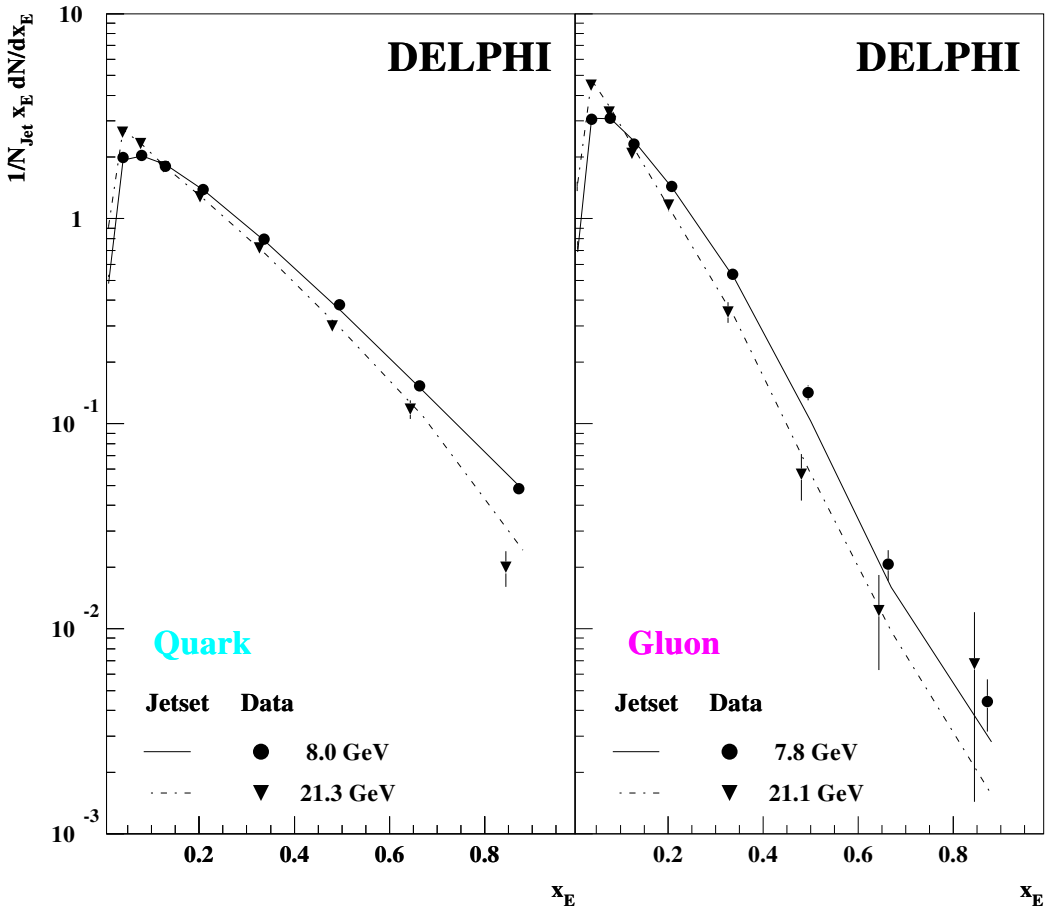

Figure 4: Scaled energy distributions for different topologies

4 Results

Sizeable differences have been observed between the scaled energy x_E-distributions of stable hadrons produced in quark and gluon jets [11, 20, 21]. In Fig. 4 the fragmentation functions for quark and gluon jets in the overall sample of three-jet events are shown for different values of κ_{DDT}. An approximately exponential decrease of the fragmentation function with increasing x_E is seen, which is more pronounced in the gluon case. The extra suppression at high x_E (by almost one order of magnitude) of gluon jets relative to quark jets is expected because, contrary to the quark case, the gluon cannot be present as a valence parton inside the produced hadron. The valence quarks of the hadrons first have to be produced in a $g \to q\bar{q}$ splitting process. The softening of the fragmentation functions with increasing κ_{DDT} is observed. This effect is more pronounced for gluon jets than for quark jets.

Fig. 5 and 6 show the quark and gluon fragmentation functions for fixed x_E as a function of the scale κ_{DDT} (in the following called 'fan' plots). The results obtained from

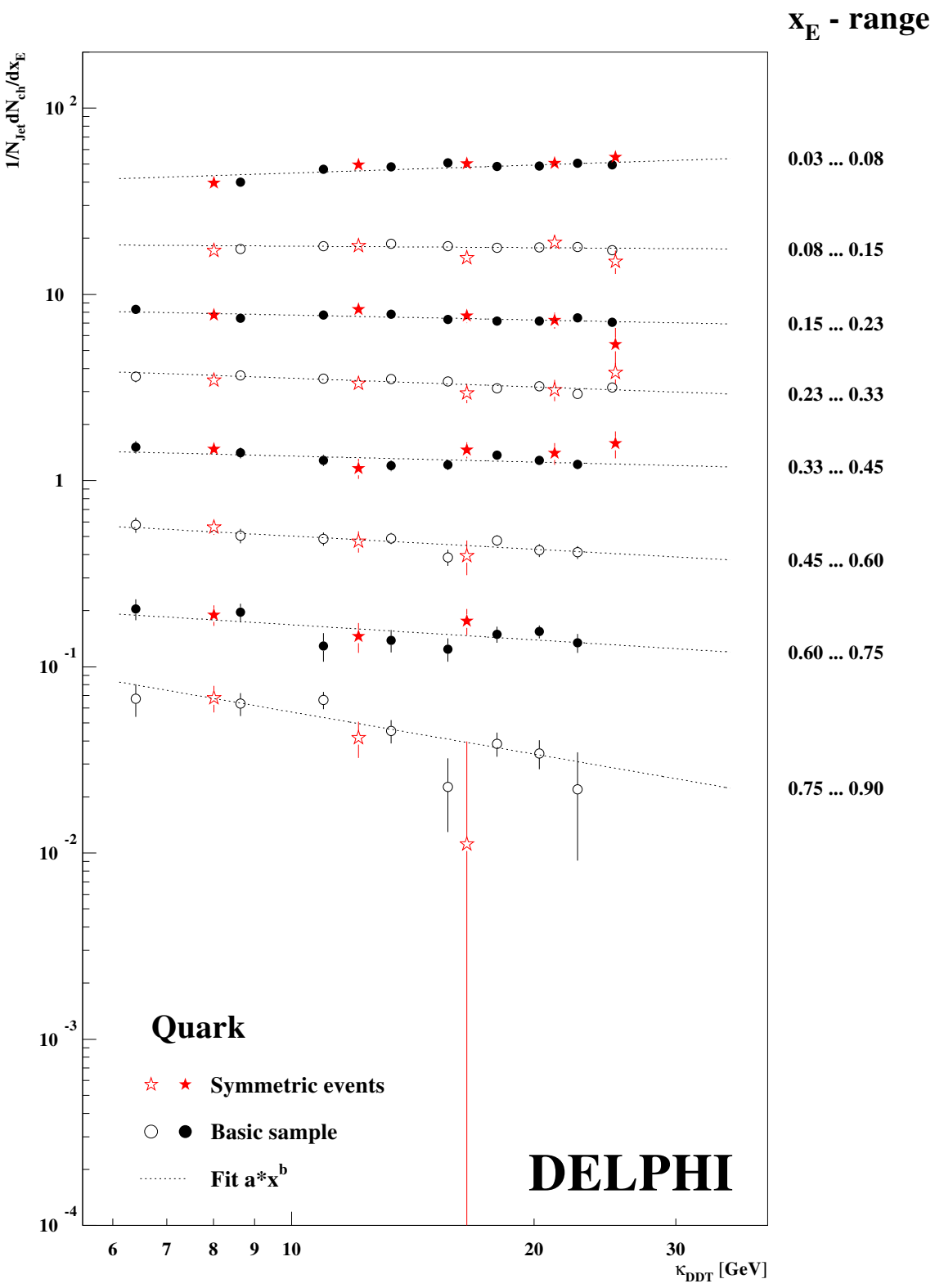

Figure 5: Scale dependence and scaling violation of the quark fragmentation functions. The dashed line is the result of a power law fit.

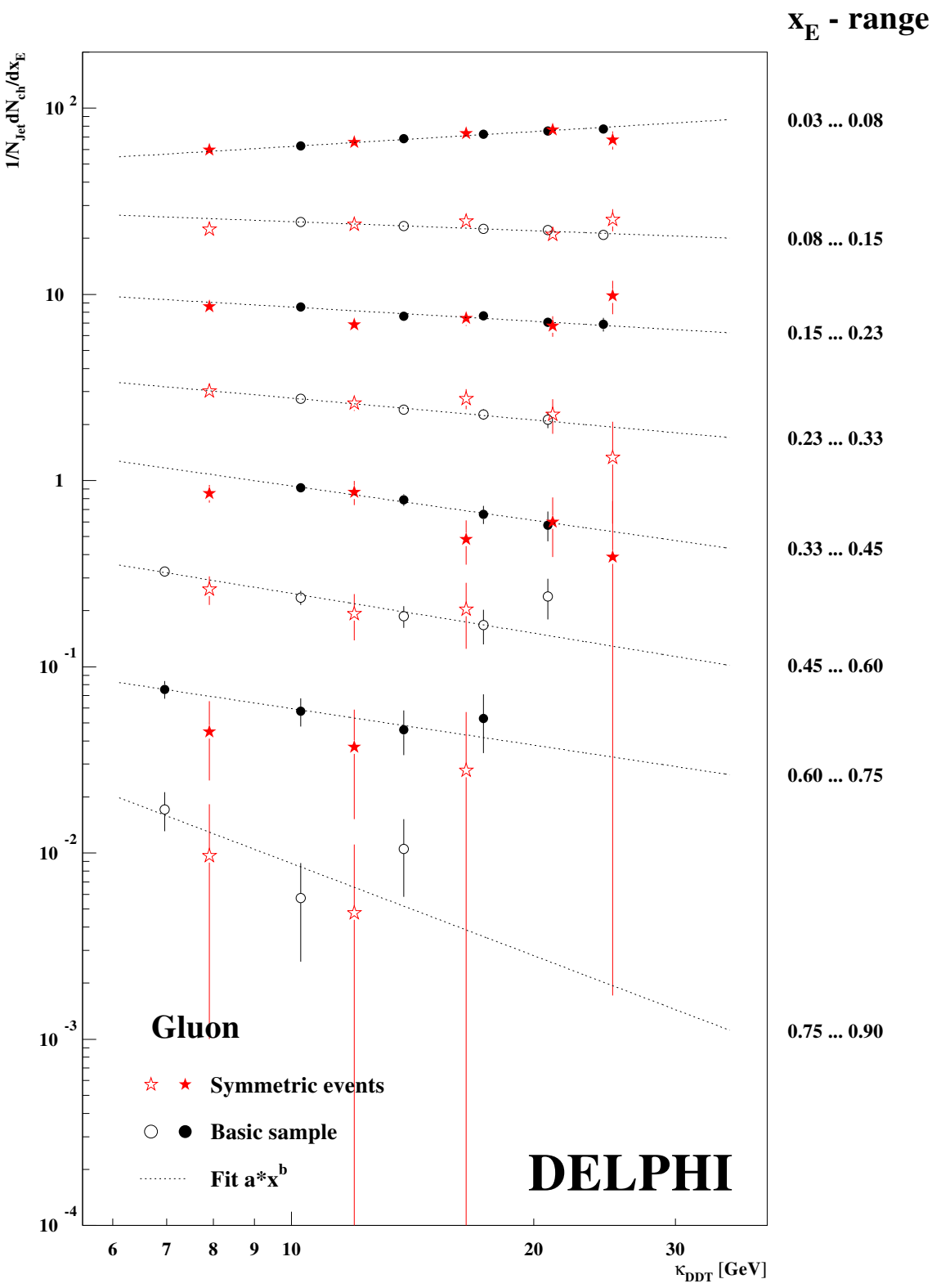

Figure 6: Scale dependence and scaling violation of the gluon fragmentation functions. The dashed line is the result of a power law fit.

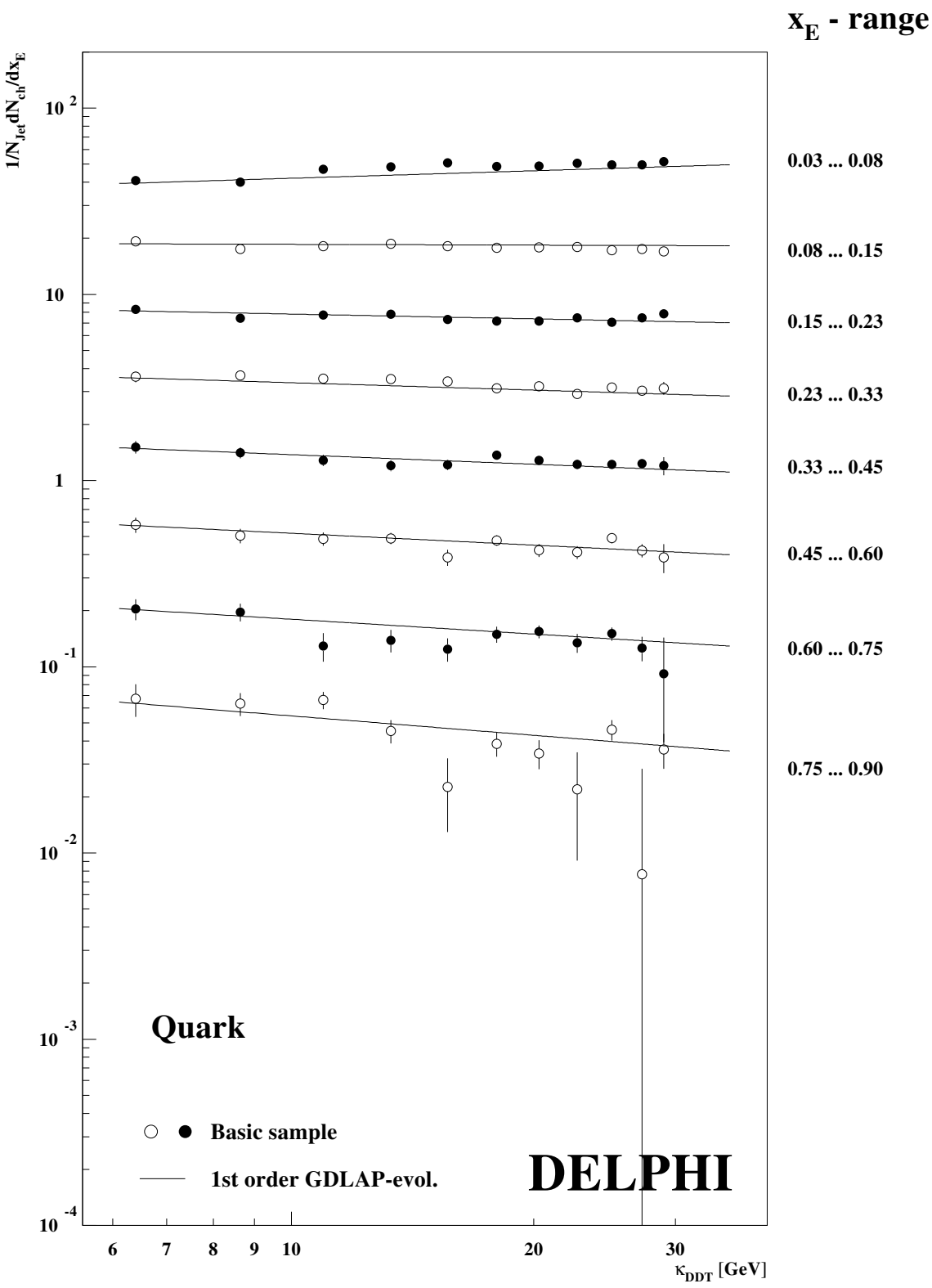

Figure 7: Scale dependence and scaling violation of the quark fragmentation functions. The full line is the expectation of the GDLAP evolution of the fragmentation function.

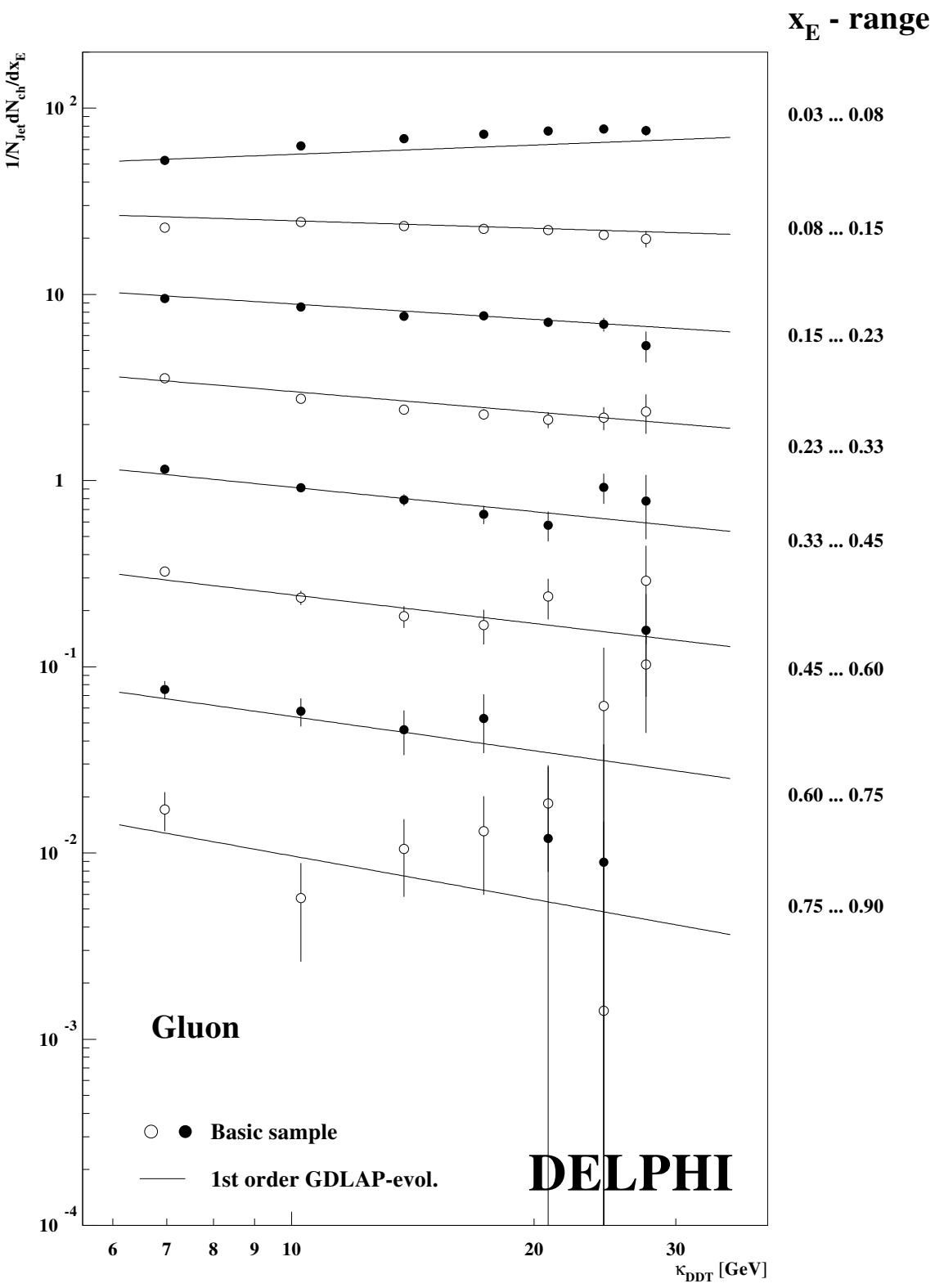

Figure 8: Scale dependence and scaling violation of the gluon fragmentation functions. The full line is the expectation of the GDLAP evolution of the fragmentation function.

the overall data set and from the symmetric events agree well. A nearly linear behaviour is observed both in the quark and gluon plot indicating a power law energy behaviour. Fits of the form:

$$D(x_E, \kappa_{DDT}) = b \cdot \kappa_{DDT}^{a}, \tag{8}$$

indicated by the dotted lines in the fan plots describe the behaviour of the data well. The behaviour typical of scaling violations is observed in both plots, namely a strong fall off at large x_E which diminishes with falling x_E, vanishes around $x_E \sim 0.1$, and finally for small x_E turns into a rise. The rise at small x_E causes the increase of multiplicity with the scale [5]. The scaling violation behaviour is much stronger for gluons than for quarks. This is expected due to the higher colour charge of gluons.

Figs. 7 and 8 show the fan plots data again. Several data points which have large systematic uncertainty, and were therefore not present in Figs. 5 and 6 and in the power law fits, are included in these plots as well as an evolution of the fragmentation functions predicted by solving the GDLAP equation. For the evolution the fragmentation functions at $\kappa_{DDT} = 9.8$ GeV have been fitted over the whole x_E range to the form of Eq. 6. The parameters of the fit are given in Tab. 3.

	Quark Jets	**Gluon Jets**
p_1	-3.08	-4.20
p_2	1.05	1.65
p_3	0.18	0.07
p_4	0.40	0.63

Table 3: Parameters of the fitted fragmentation functions.

The behaviour of the data is very well represented by the GDLAP evolution, besides for the lowest x_E range, where non perturbative effects are not negligible. This fortifies the scaling violation interpretation and is a justification of this analysis, especially of the usage of the scale κ_{DDT}.

In Fig. 9a the logarithmic slope as obtained from the fits (Eq. 8) for quarks and gluons is plotted as a function of x_E. The typical scaling violation pattern is directly evident. The data is very well represented by the GDLAP expectation for quarks and for gluons. The stronger scaling violation for gluons compared to quarks is due to the higher colour charge of the gluons. For gluons also the expectation for alternative values of C_A (2,4) is shown as a grey area, indicating that this measurement has a high sensitivity to the colour factor C_A.

In Fig. 9b the ratio of the scaling violations for quarks and gluons is shown. The expectation from the GDLAP evolution is shown as a solid line. Again, as expected (see Eq. 7), it rapidly approaches the ratio $C_A/C_F = 2.25$ at large x_E. The pole at $x_E \sim 0.1$ is due to the vanishing of the quark scaling violation in this x_E range. The measured values are nicely consistent with the QCD expectation. Within the large errors of the measurement, which are predominantly caused by the strong nonlinearity in the error propagation of the ratio, the ratio of the scaling violations for gluons to quarks directly measures the colour factor ratio:

$$\frac{C_A}{C_F} = \frac{S_g}{S_q} \mid_{x_E > 0.5} = 2.7 \pm 0.7(stat.)$$

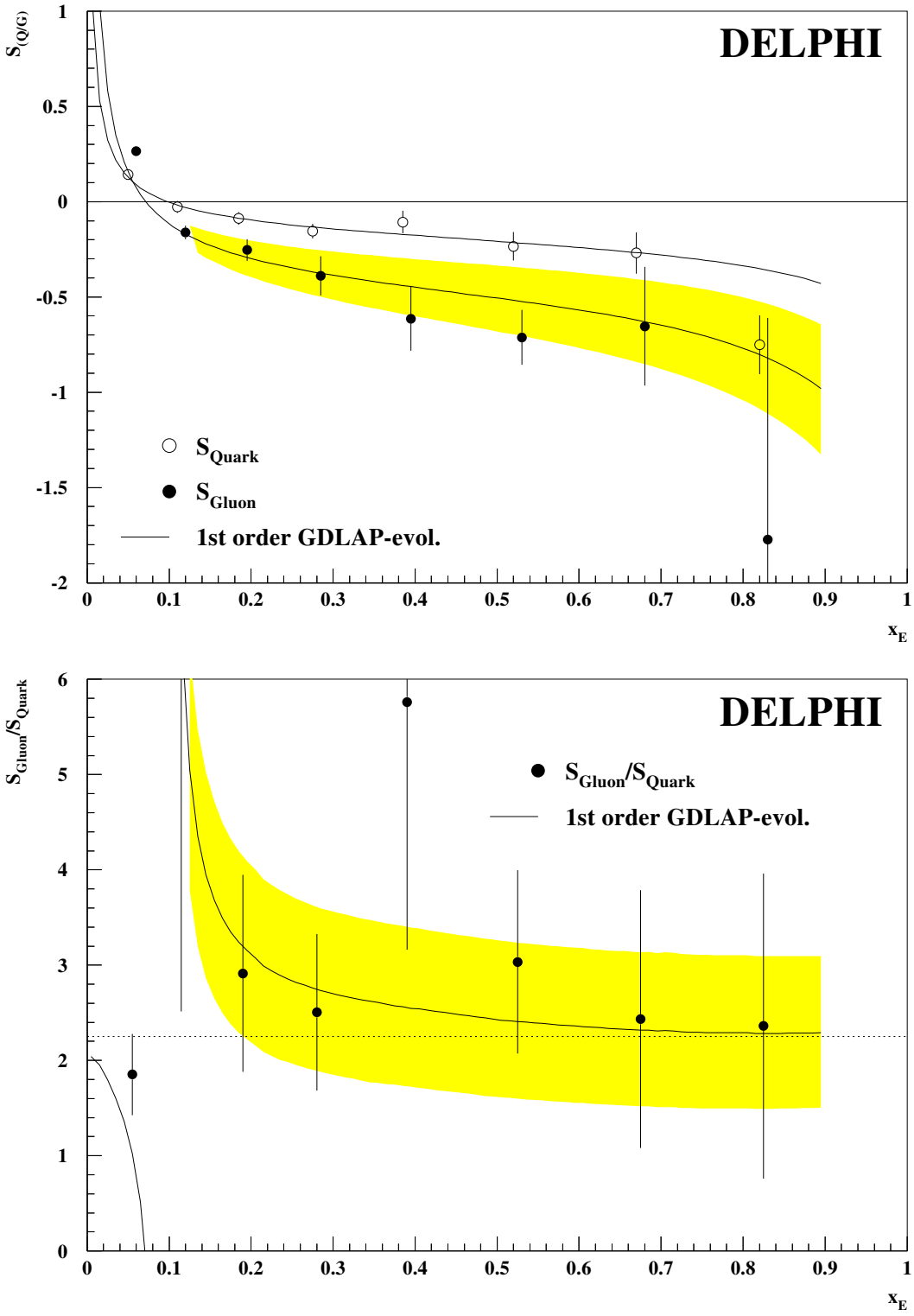

Figure 9: a) Comparison of scaling violation of quark and gluon jets (upper plot. b) Ratio of the scaling violations (lower plot). The full lines are the expectation of the GDLAP evolution. The grey areas are obtained by changing C_A in the range of 2 to 4.

5 Conclusions

Light quark jets and gluon jets of similar transverse momentum like scale κ_{DDT} have been selected from planar symmetric three-jet events measured with DELPHI. Using impact parameter techniques, gluon jets have been selected in heavy quark events, and heavy quark contributions have been depleted in a mixed quark/gluon jet sample. Properties of pure quark and gluon jets have been obtained by subtraction techniques.

A precise measurement of the quark and gluon fragmentation function into stable charged hadrons has been presented as function of the jet scale κ_{DDT}.

Scaling violations are clearly observed for quark jets as well as for gluon jets. The last presents evidence for the triple gluon coupling, a basic ingredient of QCD. Scaling violations are observed to be much stronger for gluon compared to quark jets. The colour factor ratio:

$$\frac{C_A}{C_F} = 2.7 \pm 0.7(stat.)$$

is measured from the ratio of scaling violations in gluon to quark jets.

References

[1] C. Chang et al., Phys. Rev. Lett. **35** (1975) 901.

[2] H.L. Anderson et al. Phys. Rev. Lett. **38** (1977) 1450.

[3] EMC, J.J. Aubert et al., Phys. Lett. **B114** (1982) 373,
TASSO Collab., R. Brandelik et al., Phys. Lett. **B114** (1982) 65.

[4] ALEPH Collab, CERN-PPE/97-003.

[5] DELPHI Collab., K. Hamacher, O. Klapp, P. Langefeld, S. Marti, M. Siebel et al., *The Scale Dependence of the Multiplicity in Quark and Gluon Jets and a Determination of* C_A/C_F contributed paper to the EPS-HEP Conf., Jerusalem 1997.

[6] DELPHI Collaboration, Nucl. Instr. and Methods in Physics Research **A303** (1991) 233.

[7] DELPHI Collab., K. Hamacher, O. Klapp, P. Langefeld et al. *Investigation of the Splitting of Quark and Gluon Jets*, contributed paper to the EPS-HEP Conf., Jerusalem 1997.

[8] O. Klapp, Diplomarbeit "Quark- und Gluonjets aus Z-Zerfällen — Vergleichende Studien des Jetendzustandes und der Substruktur" WU **D** 95-15 (University of Wuppertal, Germany).

[9] M. Siebel, Diplomarbeit, University of Wuppertal, Germany, 1997.

[10] S. Catani, Yu.L. Dokshitzer, M. Olsson, G. Turnrock, B.R. Webber, Phys. Lett. **B269** (1991) 432;
S. Bethke, Z. Kunszt, D.E. Soper, W.J. Stirling, Nuclear Physics **B370** (1992) 310.

[11] DELPHI Collaboration, Z. Phys. **C70** (1996) 179.

[12] T. Sjöstrand, Comp. Phys. Comm. **39** (1986) 346;
T. Sjöstrand, M. Bengtsson, Comp. Phys. Comm. **43** (1987) 367;
T. Sjöstrand, *JETSET 7.3 Program and Manual*, CERN-TH 6488/92.

[13] DELPHI Collaboration, Z. Phys. **C73** (1996) 11.

[14] The DELPHI Collaboration, *DELPHI event generation and detector simulation*, DELPHI 89-67 PROG-142.

[15] DELPHI Coll., Nucl. Inst. and Meth. **A378** (1996) 57.

[16] Yu.L. Dokshitzer, private communication;
Yu.L. Dokshitzer, V.A. Khoze, A.H. Mueller, S.I. Troyan, *Basics of perturbative QCD*, Editions Frontieres, 1991;
Yu.L. Dokshitzer, D.I. Dyakonov, S.I. Troyan, Phys. Rep. **58** No. 5 (1980) 269.

[17] L. Lönnblad, *ARIADNE 4.4 Program and Manual*, Comp. Phys. Comm. **71** (1992) 15.

[18] V.N. Gribov, L.N. Lipatov, Sov. J. Nucl. Phys., 15:438 and 675, 1972;
G. Altarelli, G. Parisi, Nucl. Phys. **B126** (1977) 298;
Yu.L. Dokshitzer, Sov. Phys. JETP **46** (1977) 641.

[19] P. Nason, B.R. Webber, Nucl. Phys. **B421** (1994) 473.

[20] OPAL Collaboration, Z. Phys. **C68** (1995) 179.

[21] ALEPH Collaboration, Phys. Lett. **B384** (1996) 353.